Available online at www.sciencedirect.com

SCIENCE DIRECT®

Lithos 77 (2004) 765–782

LITHOS

www.elsevier.com/locate/lithos

Area selection for diamond exploration using deep-probing electromagnetic surveying

Alan G. Jones*, James A. Craven

Geological Survey of Canada, 615 Booth Street, Ottawa, ON, Canada K1A 0E9

Received 25 June 2003; accepted 4 January 2004
Available online 7 July 2004

Abstract

Previously proposed methods of area selection for diamond-prospective regions have predominantly relied on till geochemistry, airborne geophysics, and/or an appraisal of tectonic setting. Herein we suggest that a novel, deep-probing geophysical technique—electromagnetic studies using the natural-source magnetotelluric (MT) method—can contribute to such an activity. Essentially, diamondiferous regions must have (1) old lithosphere, (2) thick lithosphere, and (3) lithosphere that contains high concentrations of carbon. Deep-probing MT studies are able to address all three of these. The second and the third of these can be accomplished independently using MT, but for the first the geometries produced from modelling the MT observations must be interpreted with appropriate interaction with geologists, geochemists and other geophysicists. Examples are given from the Slave and Superior cratons in North America, with a brief mention of an area of the Rae craton, and general speculations about possible diamondiferous regions.

Keywords: Magnetotellurics; Geophysics; Slave craton; Superior craton; Rae craton

1. Introduction

As diamond exploration activities proceed into frontier areas there is a critical need for an effective area selection methodology. Previously proposed methods of area selection for diamond-prospective regions have predominantly relied on till geochemistry (e.g., Griffin and Ryan, 1995; Gurney and Zweistra, 1995; Jennings, 1995), airborne geophysics (e.g., Macnae, 1995), and/or an appraisal of tectonic setting (e.g., Helmstaedt and Gurney, 1995). As discussed by Morgan (1995), regional scale geophysical methods can aid in area selection for diamondiferous provinces, and, of the available geophysical methods, magnetotellurics and teleseismics are the two methods able to "look" into the mantle and compliment each other well. They are, in fact, the only geophysical methods with true depth resolving capability of material property variations—the other methods use inference rather than direct detection. To date, teleseismics has been used predominantly to derive the geometries of sub-cratonic Archean lithospheric mantles. Herein we propose that deep-probing electromag-

* Corresponding author. Now at: Dublin Institute for Advanced Studies, 5 Merrion Square, Dublin 2, Ireland. Fax: +1-613-943-9285.
E-mail addresses: ajones@nrcan.gc.ca, ajones@cp.dias.ie (A.G. Jones).

0024-4937/$ - see front matter © 2004 Published by Elsevier B.V.
doi:10.1016/j.lithos.2004.03.057

netic studies, using the natural-source magnetotelluric (MT) technique (Jones, 1998, 1999), offer an attractive additional, and on occasion alternate, cost-effective means for rapid area selection of diamond-prospective regions.

Essentially, diamondiferous regions must have (1) old lithosphere, (2) thick lithosphere, and, what is not as appreciably discussed in the literature, (3) lithosphere that contains high concentrations of carbon. All three of these are important: lithosphere that is "young", generally taken as Proterozoic and younger, does not appear to host diamonds. Kimberlites intruded through lithosphere that is thinner than the diamond–graphite stability field will not be diamondiferous. Lithosphere that is poor in carbon content will most likely be poor in diamonds, possibly both in diamond quantity and in diamond grade.

As we will present and demonstrate in this paper, deep-probing MT studies are able to address all three of these. The second and the third can be undertaken independently by using MT alone, but for the first—old lithosphere—the geometries produced from modelling the MT observations must be interpreted with appropriate interaction with geologists, geochemists and other geophysicists, especially seismologists. We will show the results from two cratons, the Slave craton and the western part of the Superior craton, mention briefly an area of the Rae craton, and deduce areas prospective for diamond exploration based on our results.

2. The magnetotelluric technique

The magnetotelluric (MT) method is a natural-source, electromagnetic (EM) geophysical surveying technique for obtaining information about the variations in electrical conductivity in all three dimensions, both laterally and vertically. One records the time-varying EM field components, the two horizontal electric field components (*Ex* and *Ey*) and all three magnetic field components (*Hx*, *Hy* and *Hz*), typically along profiles at a number of locations on the surface of the Earth. From these time series one computes response functions (the so-called MT impedance tensors), that relate the electric and magnetic fields to each other, and these responses are then analyzed and interpreted for information about Earth structure. Older reviews of the method are given in Vozoff (1972, 1986, 1991), and Jones (1998, 1999) discusses modern MT methods and practices, especially the imaging of the continental lithospheric and asthenospheric mantle. More specialised, technical reviews are published in issues of Kluwer's journal *Surveys in Geophysics* devoted to the review papers presented at the biennial series of EM Induction Workshops (see Surveys in Geophysics volume 13, pages 305–505, 1992; volume 17, 361–556, 1996; volume 18, 441–510, 1997; volume 20, 197–375, 1999; and volume 23, 99–273, 2002).

The basic physical phenomenon that governs all EM methods is the skin-depth effect by which penetration into a medium (in this case the Earth) is a function of the resistivity of the medium and the period of the incident EM wave. The skin depth, defined mathematically in a uniform medium as the depth at which the amplitude of the wave has been attenuated by $1/e$ (approx. 37%) of its surface value, is given by

$$\delta \approx 500\sqrt{\rho T}\ \text{(m)}$$

where δ is the skin depth (in m), ρ is the resistivity of the medium (in Ω m), and T is the period (in s). Thus, the shortest periods observed in MT (0.000025 to 0.001 s, i.e., 40 to 1 kHz in frequency) give information about the near surface (top tens to hundreds of metres), whereas the longest periods (10,000 s and on occasion beyond) give information about deep structures (typically to the base of the continental lithosphere and into the asthenosphere). This is shown schematically in Fig. 1 with an *apparent resistivity* curve, deduced from the scaled squared magnitude of the electric field divided by the perpendicular magnetic field, for a simple two-layered Earth. The short periods (high frequencies) do not penetrate deeply, sensing only the top layer and thus give the resistivity of the top layer, ρ_1. The long period (low frequencies) EM waves pass through the top layer without being affected by it, and give the resistivity of the bottom layer, ρ_2. The period where the curve crosses ρ_1 gives the thickness of the top layer, h. In addition to deriving a magnitude relationship between the electric and magnetic fields, then squaring and scaling it to yield an apparent resistivity at each period, in MT one also calculates the phase difference between the two fields. This phase difference is 45° for a uniform

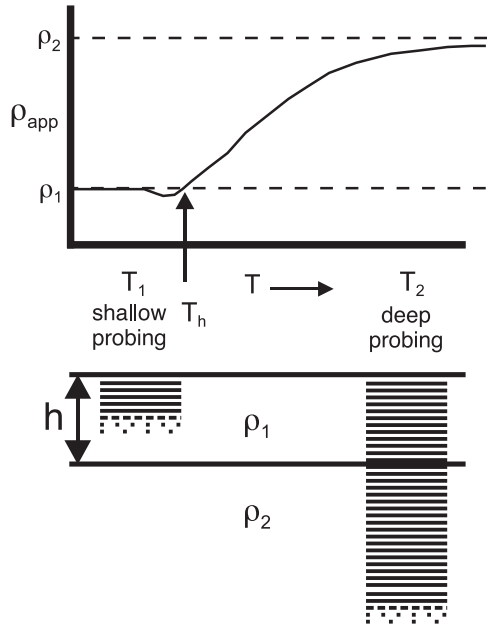

Fig. 1. Schematic apparent resistivity curve for a two-layered Earth with a less resistive layer (ρ_1) over a more resistive one (ρ_2). The apparent resistivity curve departs from the resistivity of the top layer at a period that gives the thickness of the top layer.

Earth, is less than 45° when moving to a more resistive layer with depth, and greater than 45° when moving to a conductive layer with depth.

One of MT's advantages is that exactly the same method, and almost the same instrumentation, can be used for investigations of geothermal energy resources at 100 m (e.g., Meju, 2002), mineral resources at 500–1000 m (e.g., Meju, 2002; Jones and Garcia, 2003), crustal structures to 40+ km (e.g., Jones, 1998), and lithospheric and deeper mantle to >200 km (e.g., Schultz et al., 1993; Jones et al., 2001, 2003), albeit with decreasing resolution with depth. Different magnetic sensors need to be used for the different applications, as not one single sensor exists that covers the whole period range required to image from the surface down to the base of the lithosphere.

At the low frequencies used in MT the propagating EM waves can be treated mathematically as diffusive in nature, rather than as wave propagation, and consequently MT has lower spatial resolution than most seismic methods. The MT response to a structure is the integration of the conductivity from the surface down to that structure, akin to seismic surface wave studies. However, in contrast to the small percentages of seismic impedance variations, electrical resistivity varies by over many orders of magnitude, from 0.001 Ω m and lower for graphite to 100,000 Ω m and higher for competent, unfractured silicate rock (see, e.g., Beblo, 1982; Haak, 1982), thus enabling high sensitivity to anomalous structures containing an interconnected, conducting minor phase. In addition, and in comparison to potential field methods, the MT method is not inherently non-unique; a uniqueness theorem for one-dimensional (1-D) earths, i.e., where resistivity varies with depth alone, exists (Bailey, 1970).

One-dimensional models can be fitted to the data, by objective inversion approaches, which represent minimum structure models of one sense or another. The models have either a minimum number of layers (e.g., Fischer and Le Quang, 1981) or minimum change (gradient) between many multiple layers in an over-parameterized problem (Constable et al., 1987; Smith and Booker, 1988). These two represent end-member acceptable models, and the "truth", the actual resistivity–depth distribution, lies in between. Remembering the uniqueness theorem, non-uniqueness in MT model parameter resolution is due to data inaccuracy (bias errors), imprecision (statistical errors) and inadequacy (insufficient bandwidth and insufficient estimates per decade), but not due to inherent non-uniqueness.

As well as 1-D layer-cake models of the Earth, MT data can be modelled using two-dimensional (2-D) and three-dimensional (3-D) methods, which include both forward trial-and-error approaches (e.g., Wannamaker et al., 1984, 1985) and formal inversion (e.g., deGroot-Hedlin and Constable, 1990; Smith and Booker, 1991; Siripunvaraporn and Egbert, 2000; Rodi and Mackie, 2001). Two-dimensional models are appropriate for MT data that exhibit two-dimensionality in their responses, whereas 3-D models are appropriate for array data or MT data that cannot be validly modelled using 2-D. Dimensionality validity tests are undertaken within a statistical framework that considers the effects of local, electric field distortion and also noise in the data, and yields the regional 2-D (Groom and Bailey, 1989; Groom et al., 1993; McNeice and Jones, 2001) or 3-D (Garcia and Jones, 2001) responses.

Finally, akin to seismic anisotropy revealed through teleseismic shear wave SKS studies (see Snyder et al., 2004), various workers present MT anisotropy determined qualitatively from the MT strike information

(e.g., Mareschal et al., 1995; Simpson, 2001; Bahr and Simpson, 2002). However, given the vast range of electrical conductivity, one must be careful that the EM information from different directions is coming from the same depths. We present here MT anisotropy information from a large portion of the western part of the Superior craton that is consistent with Archean tectonic processes.

3. Old lithosphere

That diamonds occur primarily in Archean regions is the well-known *Clifford's Rule* (Clifford, 1966). However, a dilemma facing diamond exploration is the development of a reasonably useful predictive model for the tectonic development of Mesoarchean lithosphere. Whereas the plate tectonic paradigm can be used as a well-established predictive exercise in mineral exploration, plate tectonics, in the modern sense, only became the dominant tectonic process by Paleoproterozoic times, although some are appealing to it to explain Neoarchean events (e.g., Davis et al., 2003; White et al., 2003). In Paleoarchean times it has been suggested that plate tectonics, sensu stricto, was not the dominant tectonic process (articulated most recently by Bleeker, 2002), and the transition between the dominance of plume or sagduction (e.g., Davies, 1992; Hamilton, 1998) tectonics over plate tectonics must have occurred as the mantle became more ordered and less chaotic, likely during the Mesoarchean. The conundrum is that many diamonds are reported to be dated as Mesoarchean in age, so their search is compounded by this difficulty in defining an appropriate predictive model.

Geometries of structures imaged by EM studies within the sub-continental lithospheric mantle aid in the development of a model for the tectonic history of the craton, which relates to its age. This has been demonstrated for the Slave craton, the western part of the Superior craton, and part of the Rae craton, and is discussed in greater detail below for each of these.

4. Thick lithosphere

Diamonds only exist stably in thick, cold lithosphere at depths where the continental lithosphere–asthenosphere transition, taken typically as an isotherm of about 1300 °C denoting a change from a conductive geotherm to convective geotherm (e.g., Jaupart and Mareschal, 1999), lies below the graphite–diamond stability field. In the absence of any interconnected conducting material, the sub-continental lithospheric mantle (SCLM) is electrically highly resistive. Laboratory studies of the resistivity variation with temperature of mantle materials, olivine, orthopyroxene and clinopyroxene, show that resistivity values of many hundreds to tens of thousands of ohm-metres are to be expected (Xu et al., 2000), decreasing with increasing temperature. This variation is shown in Fig. 2 for those three minerals, calculated from the formulae in Xu et al. (2000) using the values shown in the figure for each mineral in the solid-state Arrhenius equation (see Xu et al., 2000, for explanation). Using appropriate mixing relationships, it is possible to determine the resistivity of the mantle for any given mineral modal composition (Ledo and Jones, 2003), and Ledo and Jones (2003) show an application for a region of the Yukon known to have harzburgitic lithospheric mantle. Using minimum resistivity estimates for the upper mantle of 5000 Ω m and the observed harzburgitic mineralogy, Ledo and Jones (2003) deduce a maximum possible temperature

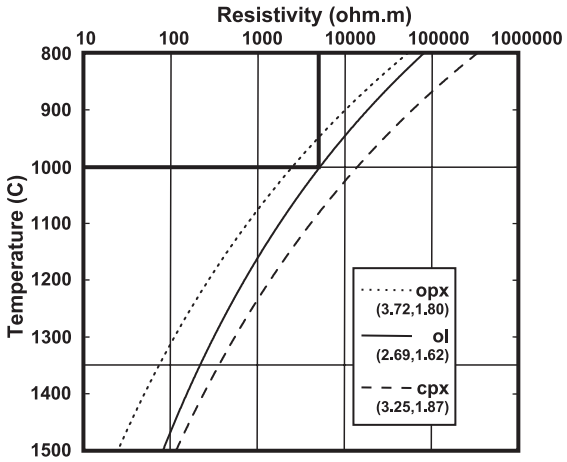

Fig. 2. Resistivity–temperature curves for olivine, Opx and Cpx mineralogies based on laboratory measurements in Xu et al. (2000). The numbers given for each mineralogy are the pre-exponent term ($\log_{10}(\sigma_0)$, where σ_0 is in S/m) and activation enthalpies (exponent term, ΔH, in eV) respectively in the Arrhenius equation for conductivity given by $\sigma = \sigma_0 \exp(-\Delta H/kT)$, where k is Boltzmann's constant and T is the temperature in Kelvin.

of 1000 °C, and a less-well defined minimum temperature of 850 °C, for the Intermontane Belt.

MT can determine the thickness of the lithosphere, i.e., the depth to the lithosphere–asthenosphere boundary (LAB), due to the two orders of magnitude increase in electrical conductivity at the onset of partial melt. Sensitivity to the onset of partial melt is shown in Fig. 3 derived from the melting experimental data in Schilling et al. (1997) and Partzsch et al. (2000). The figure shows the results of heating experiments on a sample of pyroxene granulite—not a mantle rock but illustrative of the effect. At low temperatures (<1050 °C), the material conducts electric currents by the flow of electrons, and this can be described by the solid-state Arrhenius equation. At high temperatures (>1100 °C) ionic conduction becomes dominant and can be described by an appropriate mixing law.

Between these two, in the transition zone where partial melt is low (<2%), both mechanisms are important and resistivity decreases by over 1.5 orders of magnitudes within 50 °C. Quenching studies show that the melt becomes interconnected, which is critical for reducing electrical resistivity, at very low partial melt fractions. Minarik and Watson (1995) and Drury and Fitz Gerald (1996) both demonstrate that interconnectivity can be achieved with partials melts below 0.1%.

It should be appreciated that these laboratory experiments are very difficult to perform; the results

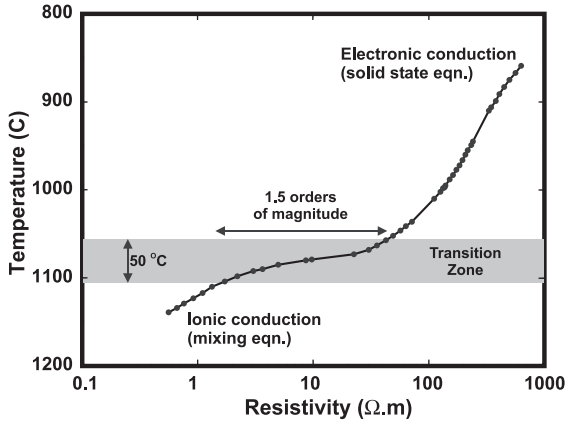

Fig. 3. Variation of resistivity of pyroxene granulite with increasing temperature as the rock is taken through partial melt. Based on the data of Schilling et al. (1997) and Partzsch et al. (2000).

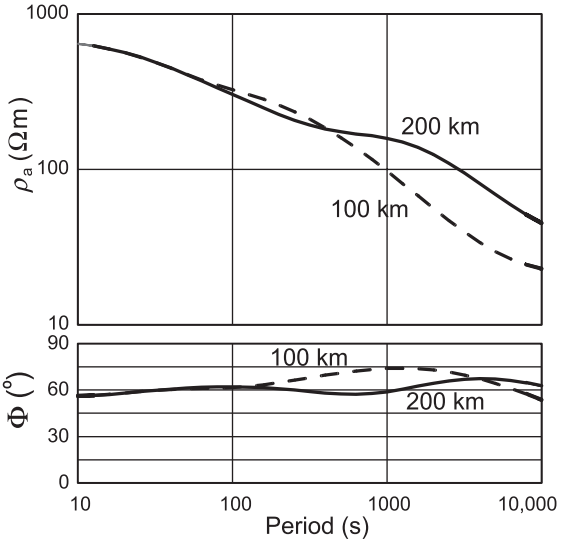

Fig. 4. Apparent resistivity and phase responses for a standard continental lithospheric mantle (see Fig. 5) with the base of the lithosphere at 200 km (full lines) and 100 km (dashed lines).

of Schilling et al. (1997) and Partzsch et al. (2000) required holding the temperature constant for 200 h to obtain a stable result at each data point. Accordingly, there are no studies of appropriate mantle rocks being taken from solid to partially molten.

Such high sensitivity to the onset of partial melt, with resistivity decreasing by over 1.5 orders of magnitude over a temperature range of less than 50 °C, means that precise MT data have the highest potential precision of any geophysical method to the depth to the LAB. This boundary is generally taken to have a temperature in the region of 1250–1350 °C (1280 °C, McKenzie and Bickle, 1988; 1250–1350 °C, Ryan et al., 1996), so the resistivity is expected to decrease from some hundreds of Ω m to about 10 Ω m over some 25 km in depth (which is equivalent to a temperature increase of around 50 °C).

Fig. 4 shows the effect on the apparent resistivity and phase curves when the depth to the LAB is changed from 200 to 100 km. Note in particular the phase responses in the 100–1000 s band of periods. The shallower LAB has higher phases than the deeper one.

As an example of LAB determination using MT, Fig. 5 shows the data, and corresponding 1-D layered Earth model, for a site near Kiruna in northern Sweden (Jones, 1982). The LAB is estimated to be

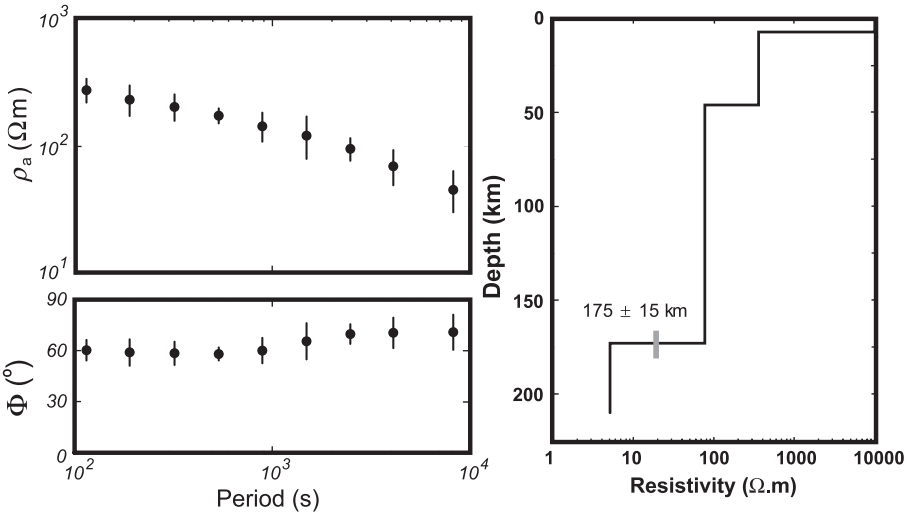

Fig. 5. EM responses from Kiruna, northern Sweden, expressed as MT parameters, plus the best-fitting 1-D model.

at a depth of 175 ± 15 km, which correlates excellently with lithospheric thickness estimates derived from seismic surface waves studies (Calcagnile, 1982, 1991; Calcagnile and Panza, 1987).

In 1977, Alekseyev et al. (1977) produced maps of the Former Soviet Union showing properties of the asthenosphere deduced from seismological and electromagnetic experiments. The maps are reproduced in Fig. 6, and demonstrate that electrical and seismological properties spatially correlate.

Accordingly, the MT method can detect whether the LAB exceeds the graphite–diamond (G–D) stability field, or not.

5. Presence of carbon

There are many candidates that can be introduced into mantle rocks for reducing electrical resistivity, and these are discussed below. For both the Slave and Superior conductors (discussed below), we exclude all of them with the exception of interconnected carbon on grain boundaries or in conducting graphite form. Carbon is highly unusual in that it can exhibit extremely low resistivity in one form, and extremely high resistivity in another. When in graphite form the carbon atoms have one *S* orbit electron and two *P* orbit electrons, and the atoms form themselves into a lattice with triagonal planar symmetry with a low energy barrier between the valence band and the conduction band. Besides the other petrophysical properties that this structure possesses, graphite has conductivity (inverse of resistivity) of 10^4 S/m (10^{-4} Ω m resistivity) across the layers, and 10^{10} S/m (10^{-10} Ω m resistivity) along the layers. In stark contrast, when carbon is in diamond form it has one *S* orbit electron and three *P* orbit electrons, and the atoms are arranged in a lattice with tetrahedral symmetry with a very high energy barrier between the valence and conduction bands. Consequently, the conductivity of diamond is 10^{-12} S/m (10^{12} Ω m resistivity).

In the sub-continental lithospheric mantle, above the graphite–diamond (G–D) transition, an interconnected graphite phase decreases electrical resistivity by two or more orders of magnitude over that predicted from laboratory studies and petrophysical modelling for an olivine or pyroxene mineralogy dominant upper mantle. Below the G–D transition, carbon exists in the form of diamond, and is highly resistive, and thus invisible, unfortunately, to EM observations.

6. Application to the Slave craton

Deep-probing magnetotelluric studies have been conducted on the Slave craton since 1996 as part of a number of programs (Jones et al., 2001, 2003). The

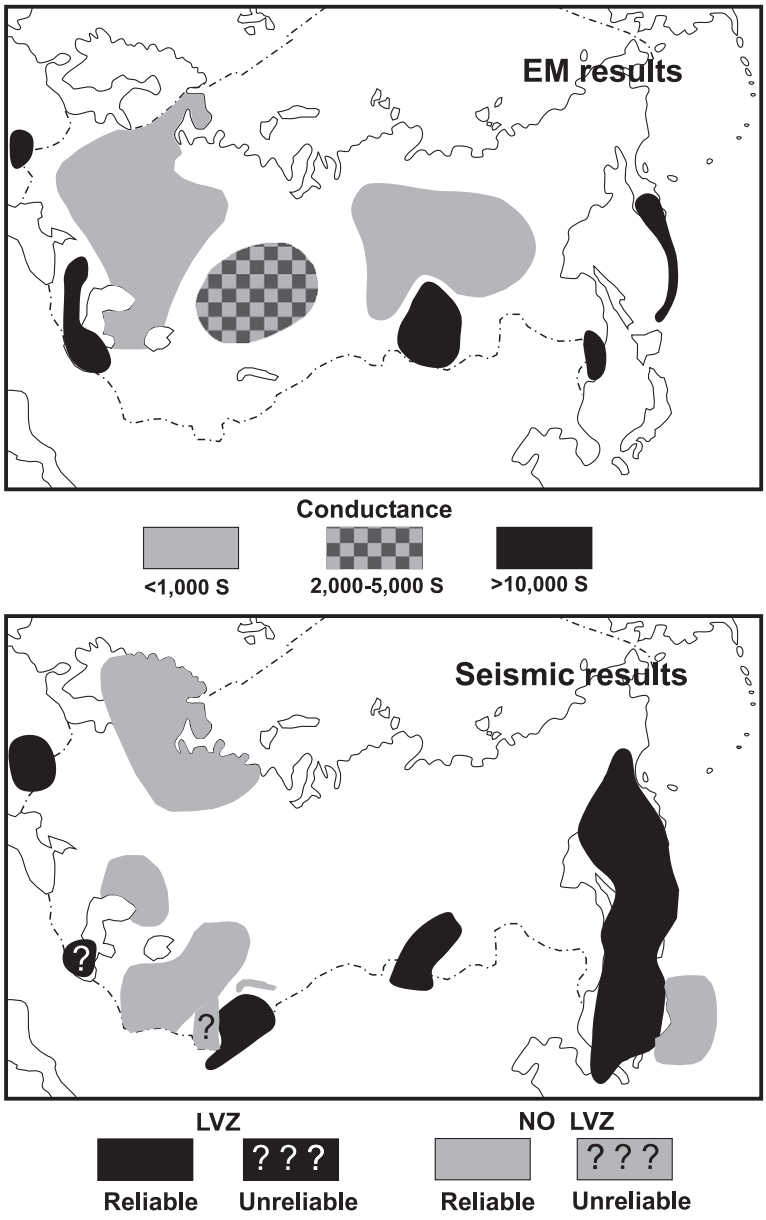

Fig. 6. Comparison of EM and seismological observations of parameters of the asthenosphere in the Former Soviet Union. Regions of high conductance for the asthenosphere correlate spatially with regions of observed seismic low velocity zones. Similarly, regions of low conductance correlate with regions where the LVZ is absent. Re-drawn from Alekseyev et al. (1977).

locations where MT data have been acquired are shown in Fig. 7 with reference to the important kimberlites, the isotope boundaries of Thorpe et al. (1992) and Davis and Hegner (1992), and the G-10 garnet lines of Grütter et al. (1999). MT coverage is greatest in the southwest part of the craton, and lowest in the northern third with only the four lake-bottom sites providing information.

Averaging the responses from all sites together, and scaling to account for local distortion effects,

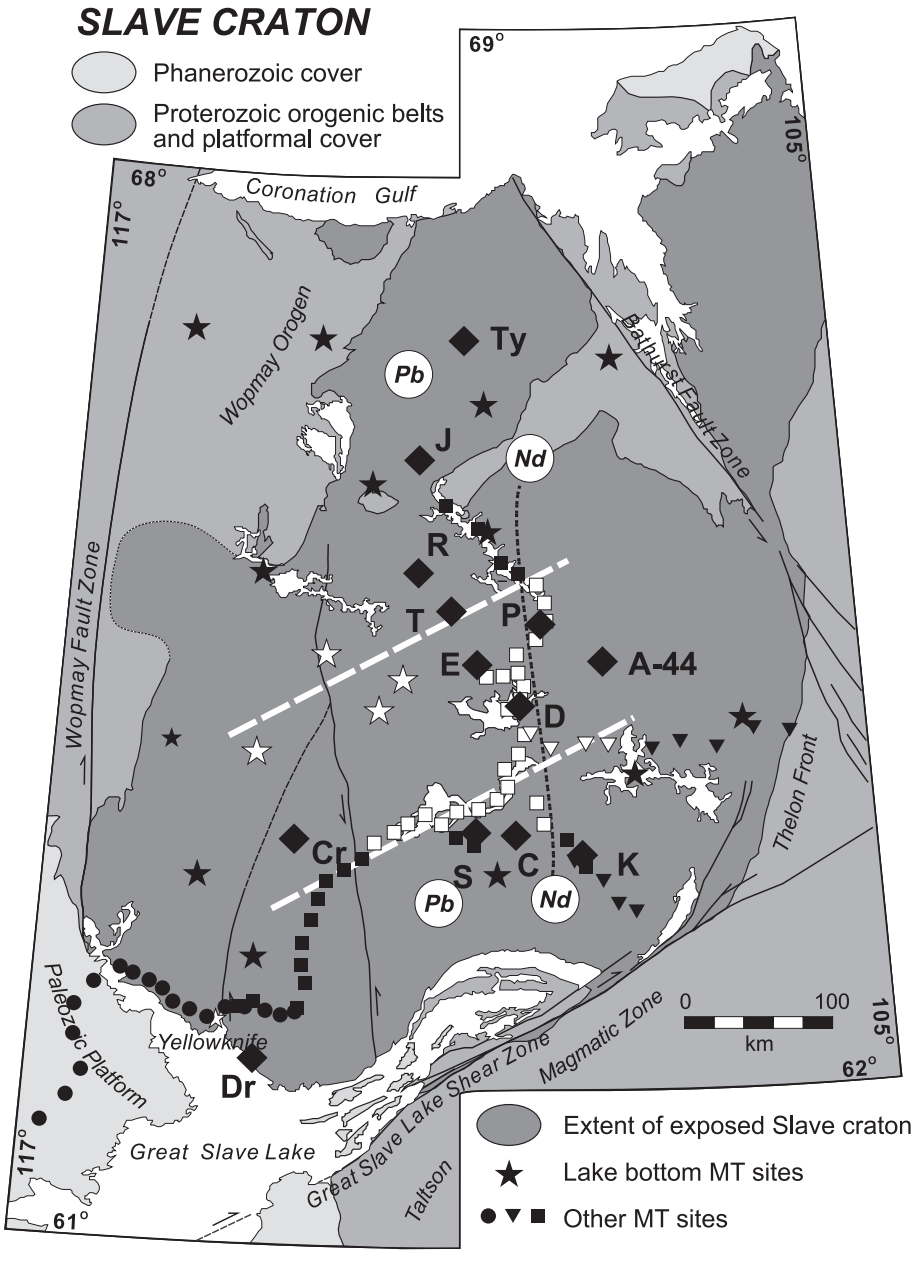

Fig. 7. Locations of magnetotelluric sites on the Slave craton, northwestern Canada. Dots: 1996 survey. Squares: 1998, 1999 and 2000 winter road surveys. Inverted triangles: 2001 Targeted Geoscience Initiative survey. Stars: 1999–2000 and 2000–2001 lake bottom locations. Open symbols show sites interpreted to be on top of the Central Slave Mantle Conductor. White dashed lines: G10 boundaries of Grütter et al. (1999). Pb and Nd isotope lines taken from Thorpe et al. (1992) and Davis and Hegner (1992). Diamonds: Important kimberlites: Ty—Tenacity; J—Jericho; R—Ranch; T—; P—Point Lake; E—Ekati; D—Diavik; A—44; K—Kennady; C—Camsell; S—Snap; Cr—Cross Lake; Dr—Drybones.

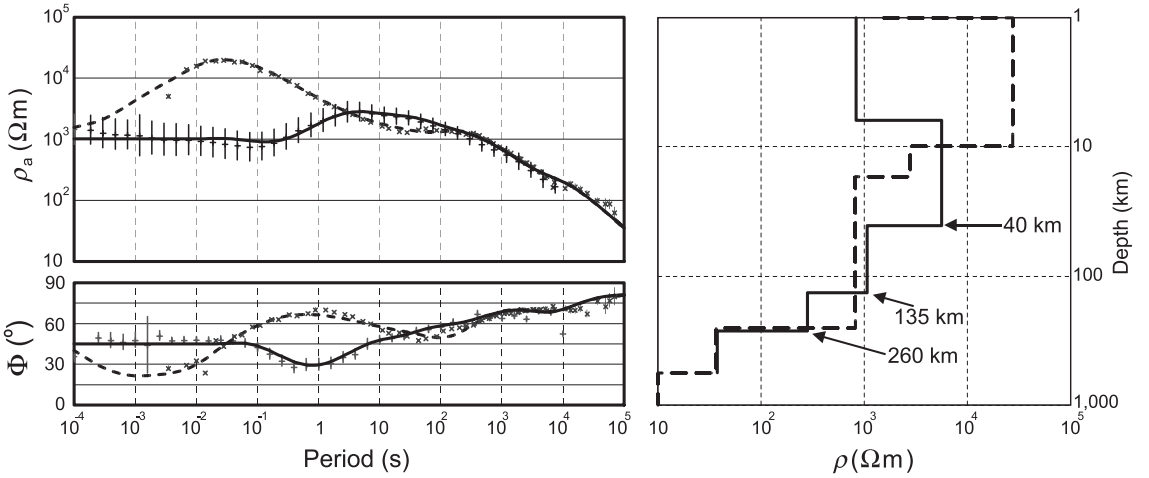

Fig. 8. Solid lines: Averaged Slave craton MT responses and 1-D best-fitting minimum layers model. Dashed lines: MT data from the central part of the Superior craton (Schultz et al., 1993) and best-fitting 1-D model.

yields the overall Slave MT apparent resistivity and phase responses shown in Fig. 8 (more details are given in Jones et al., 2003). The 1-D model that fits these data with the minimum number of layers is also shown in Fig. 8, and comprises a two-layered crust over a two-layered mantle lithosphere of thick-

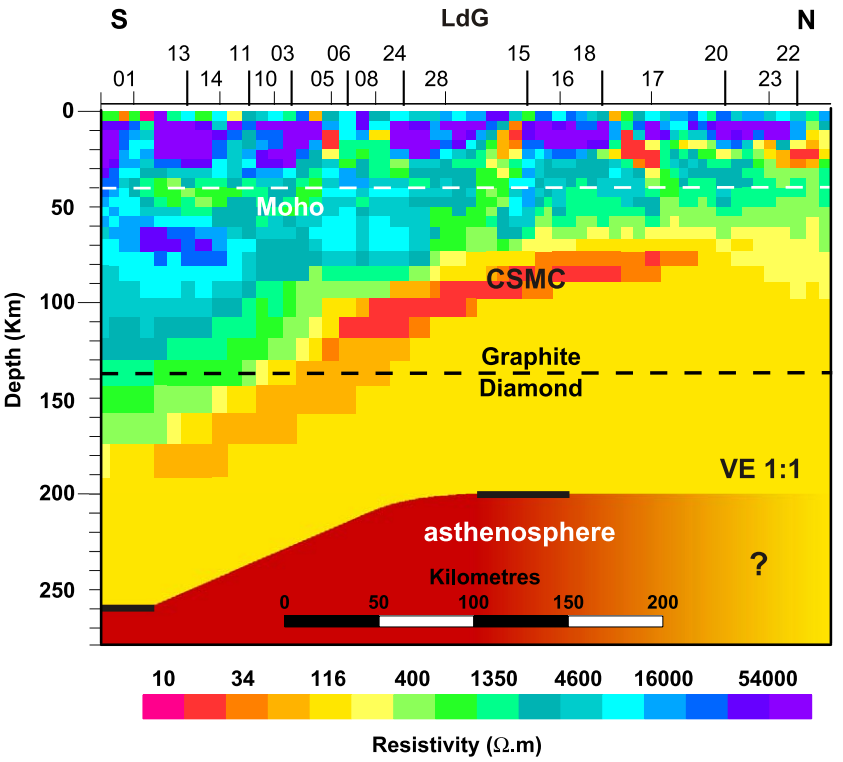

Fig. 9. Best-fitting 2-D N–S model of the winter road data from the Slave craton. LdG = Lac de Gras. CSMC = Central Slave Mantle Conductor. The depths to the base of the lithosphere are given by 1-D inversions. Taken from Jones et al. (2003).

ness 260 km. The base of the crust at 40 km was a fixed parameter in the inversion, given the sharp and distinct resistivity change at Moho depths noted by Jones and Ferguson (2001). The intra-mantle lithosphere discontinuity at 135 km approximately correlates with the graphite–diamond stability field, but it is weakly resolved and the resistivity change is in the wrong direction. The base of the lithosphere at 260 km is one of the well-resolved model parameters, but nevertheless has a rather large statistical error of ± 50 km given the large error estimates for the averaged data. A thickness of 260 km for an average dominated by southern Slave sites correlates well with the thickness of 260 km derived petrologically by Kopylova et al. (2001) from xenolith material recovered from the Kennady kimberlite (K in Fig. 7).

Comparing the averaged Slave MT response with the most accurate and precise MT response determined for any craton, namely the central part of the Superior craton (Schultz et al., 1993), shows an astounding and remarkable similarity at periods greater than about 300 s. Both the apparent resistivity curves and the phase curves from the two cratons are within each other's statistical error bounds. The 1-D model derived from this part of the Superior craton also exhibits a lithospheric thickness of 260 km, but with a far higher precision (± 20 km). That these two both display the same electrical lithospheric thickness attests to physical process limits on the maximum thickness of Archean lithosphere.

A 2-D North–South model, derived from the data along the Lupin mine winter road, is shown in Fig. 9. The prominent feature of the model is the detection of a zone of low resistivity beneath the Lac de Gras kimberlite region at depths of some 80–120 km. This Central Slave Mantle Conductor (CSMC) lies within the graphite stability field. 2-D models were also constructed along the other profiles (see Jones et al., 2003), and the stations that lie directly above the CSMC are shown in Fig. 7 in open symbols, and a plan of the CSMC is shown in Fig. 10. Note in Fig. 10 that the eastern limit of the CSMC along the profile directly east of Lac de Gras correlates spatially

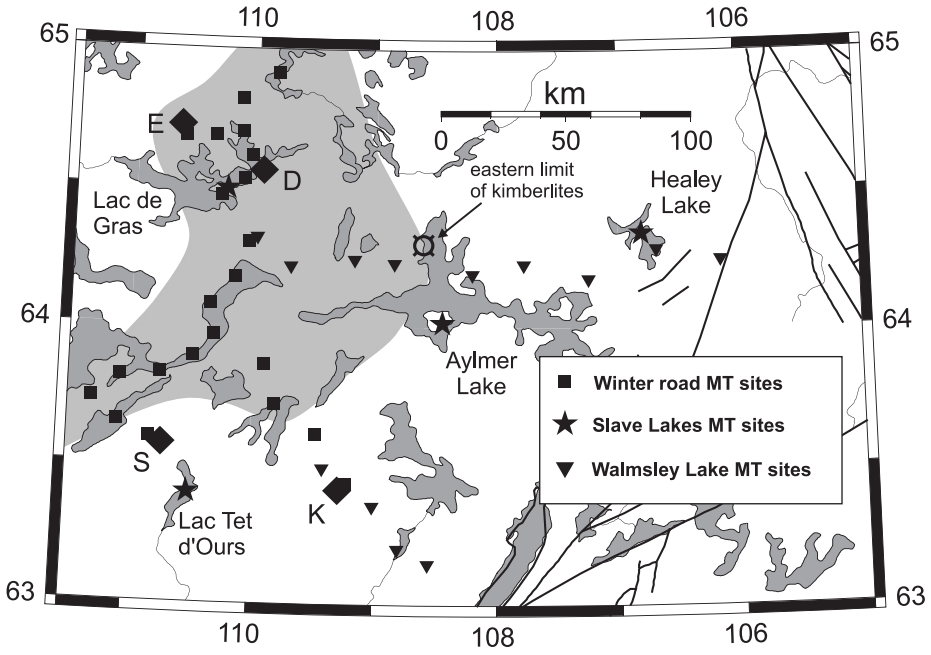

Fig. 10. Eastern boundary of the Central Slave Mantle Conductor compared to the known eastern limit of Eocene kimberlites. MT sites from the different MT surveys are depicted with different symbols. The stars represent the locations of Ekati (E), Diavik (D), Snap Lake (S) and Kennady Lake (K).

precisely with the eastern limit of Eocene kimberlites in the northern arm of Aylmer Lake.

A 3-D model of the data has been constructed, and a depth slice at 111 km is shown in Fig. 11. The CSMC can be seen to be NE–SW trending. Slices at deeper depths (not shown) imply a NW dip to the anomaly.

MT sites on the CSMC are shown in Fig. 7 as open symbols, and the spatial correlation with Grütter et al.'s (1999) G10 garnet boundaries is clearly evident. Note that the CSMC does not respect the N–S trending isotope boundaries, but, as with Grütter's lines, crosses them at a sharp angle. Also, the conductor correlates spatially and in depth extent with an ultra-depleted mantle region mapped by Griffin et al. (1999).

Based on xenolith studies from northern, central and southern Slave (Kopylova et al., 1997, 2001; Pearson et al., 1999), the expected temperatures at 80–100 km depths are 700–750 °C, which, by reference to Fig. 2, suggests an ambient resistivity of the order of >30,000 Ω m is to be expected, as is seen in the southern part of the Slave craton (Fig. 9). In contrast, the CSMC has a resistivity <15 Ω m (Jones et al., 2003). The modelled 3-D geometry of this body, with a NE–SW strike and a NW dip, was one of the key geometric factors used by Davis et al. (2003) in their argument for proposing that the SCLM beneath

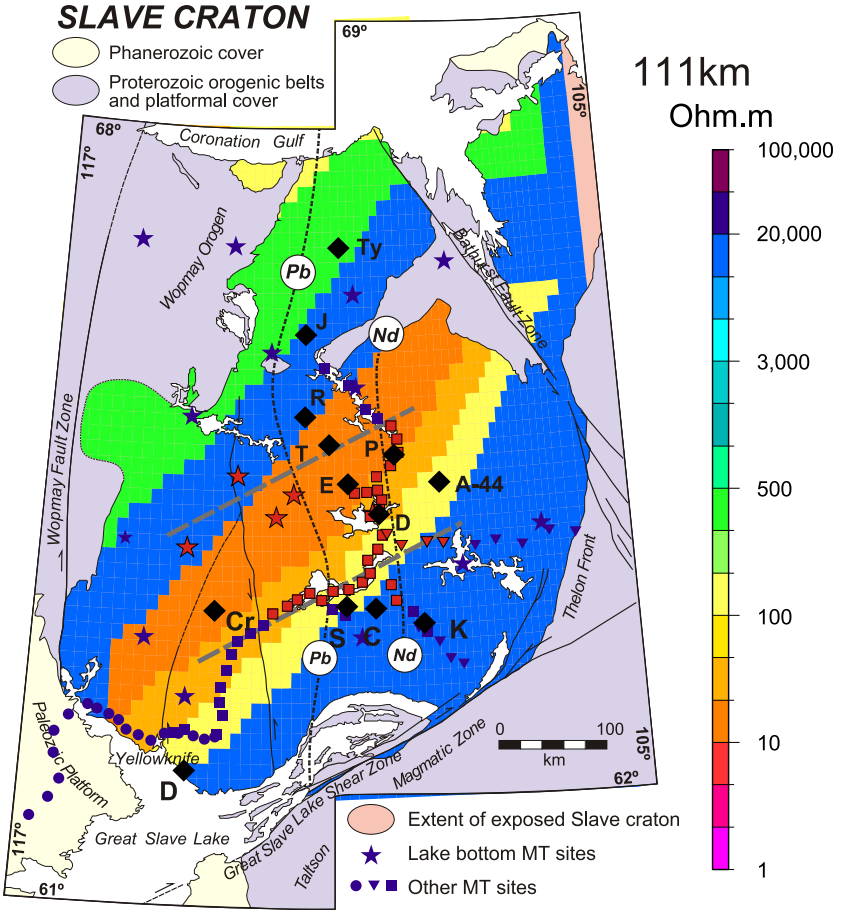

Fig. 11. Depth slice at 111 km of the 3-D resistivity model of the Slave craton. The colours on the Archean parts of the craton are the model resistivities at 111 km depth, with highly resistive (50,000–100,000 Ω m) in dark brown to highly conductive (1 Ω m) in red. The MT site locations are shown with different symbols for the different surveys, and the model is best constrained in regions of high site density.

the Slave today is not the original SCLM formed during Mesoarchean time. Davis et al. (2003) postulate that the Slave's SCLM is the consequence of subcretion of exotic lithosphere during an orogenesis at 2630–2590 Ma, postdating final Slave crustal amalgation at 2690 Ma.

7. Application to the Superior craton

In the western part of the Superior craton, Craven et al. (2001) have discovered distinctive electrical anisotropy over a wide region. An example is shown in Fig. 12 of the apparent resistivity and phase curves from two orthogonal directions from a representative site in the southern part of the region. Note that the short period responses are the same, testifying to the 1-D nature of the crust. With increasing period, the two responses diverge, indicative of either intrinsic anisotropy or structural anisotropy.

The strengths of electrical anisotropy, given by the maximum phase difference in the two orthogonal directions, and the directions of maximum conductivity are shown in Fig. 13. Three zones are apparent, and representative MT phases from each zone are shown in Fig. 14. The northern zone (yellow arrows and sites) exhibits NW–SE trending anisotropy that includes the lower crust and lithospheric mantle. The middle zone (green arrows and sites) exhibits very low phase differences, indicative of 1-D structure. The southern zone (blue arrows and sites) exhibits E–W trending anisotropy of the lithospheric mantle only.

Models of the data show an isotropic conducting body beneath the central zone within the SCLM that displays the same properties as the body in the central Slave craton. This conductor lies within the North Caribou Terrane (NCT), a Mesoarchean terrane within the mélange of predominantly Neoarchean terranes that form the western region of the Superior craton. The two bounding regions that display high anisotro-

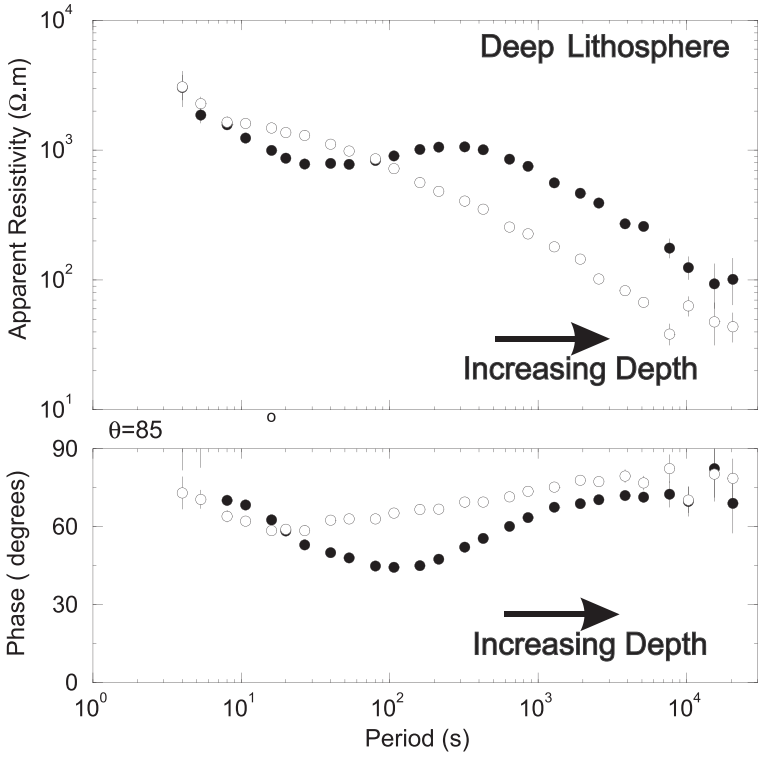

Fig. 12. MT apparent resistivity and phase data from a site in the southern region of the western Superior craton. The full symbols are those in a direction of N85E, and the open symbols perpendicular to that, i.e., N05W.

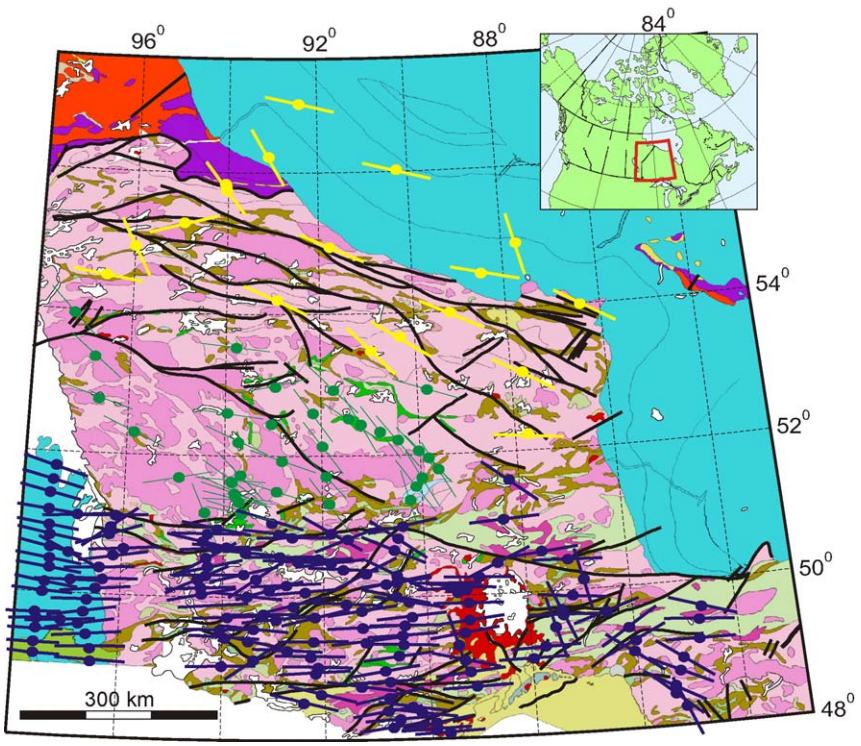

Fig. 13. Electrical anisotropy for western Ontario and eastern Manitoba, Canada, in the western Superior craton. The data fall into three groups: a northern group (yellow) with a strike of NW–SE. A central group (green) virtually 1-D. A southern group (blue) with a strike of E–W. Also shown on the figure are major faults in the region.

py have electrical strike directions parallel to the major syn- and post-Kenoran zones of transpression on either side of the NCT.

8. Application to the Rae craton

A low resolution MT experiment across Baker Lake, Nunavut, northern Canada, crossed the Rae–Hearne boundary designated by the Snowbird Tectonic Zone (Jones et al., 2002). The data yielded crustal and mantle information that addressed the Neoarchean geometry of Rae–Hearne collision. Of particular note is that despite regionally extensive and pervasive Proterozoic metasomatism (Cousens et al., 2001) the Rae craton lithospheric mantle is highly resistive and can be explained by the dry mineralogies represented in Fig. 2. This observation is counter to the suggestion of Boerner et al. (1999) that metasomatism will induce enhanced conductivity. Thus, although the lithosphere in this location is undoubtedly old and thick, it does not contain any measurable amount of interconnected graphite. By induction, this would suggest that there are unlikely to be significant diamonds within kimberlites that came through this region.

9. Cause of conductivity enhancement and redox conditions

Given our understanding of the conductivity of olivine from laboratory studies (Xu et al., 2000), some features in our models are too conductive, by 2–3 orders of magnitude, for an olivine-dominant mantle without the addition of an interconnected minor conducting phase. Such differences are often attributed to interconnected water or free H+, partial melt phases, grain boundary carbon, carbon in the form of graphite

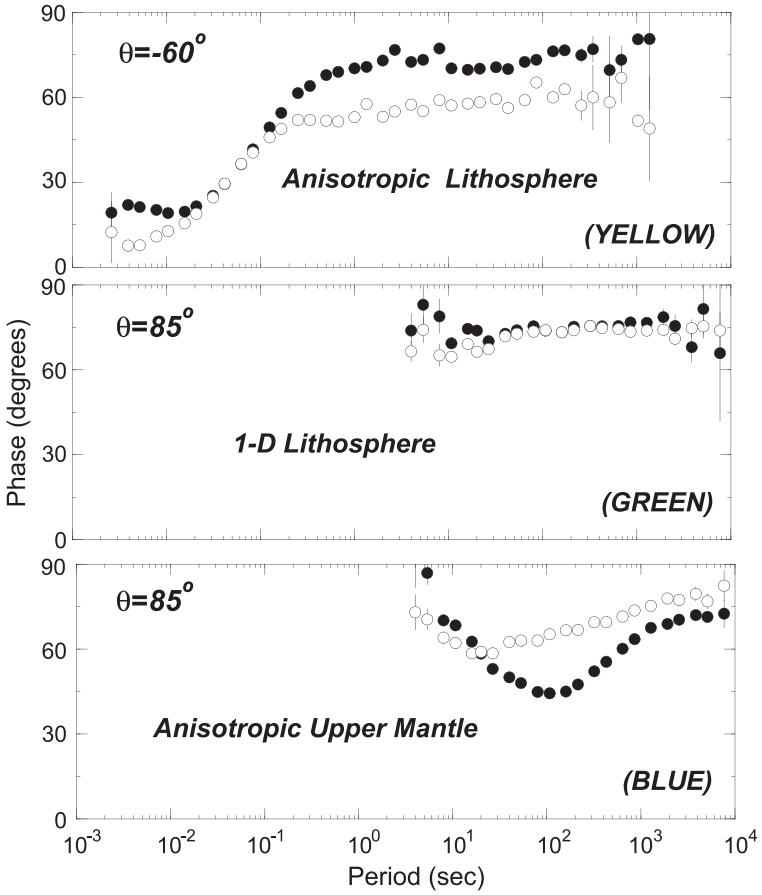

Fig. 14. MT phase data from three representative sites in the three regions shown in Fig. 13.

or sulphides within the upper mantle (for discussion see Constable and Heinson, 1993).

The observation of >0.03 S/m material within continental upper mantle requires olivine water contents of the order 1000 H/10^6 Si (Hirth et al., 2000). Such an amount of water may be tenable at sub-Moho depths if the olivine *a*-axis is strongly aligned within a region. The alignment of the *a*-axis would imply a strongly anisotropic conductor with the anisotropic axes aligned with the teleseismic fast direction. These correlations cannot be made easily for either the central Slave where the CSMC is isotropic, nor for the Superior where the electrical anisotropy is oblique to the observed teleseismic SKS anisotropy fast directions (Kay et al., 1999).

Partial melting enhances conductivity due to the high mobility of charge carriers within a melt fraction; however, it is unlikely such shallow zones of partial melt exist as heat flow values at the surface of the Slave craton (Lewis and Hyndman, 1998) and Superior Province (Jaupart and Mareschal, 1999) are low, and petrological estimates of geothermal gradient also infer thick cold lithosphere as recently as the Eocene (Russell and Kopylova, 1999; MacKenzie and Canil, 1999; Russell et al., 2001).

Sulphides are a recent suggestion as a cause for upper mantle conductivity (Ducea and Park, 2000): sulphides have electrical conductivities in the range 10^2–10^6 S/m. Interstitial sulphides are observed in quantities as high as 330 ppm in xenoliths from the Kaapvaal craton (Alard et al., 2000), but they would have to be almost perfectly interconnected to result in a conductivity of the order of 0.05–0.1 S/m, and be interconnected over the large areas we observe in our

two study areas. In addition, the CSMC correlates laterally and in depth with an ultradepleted region mapped by Griffin et al. (1999).

Grain boundary carbon may also contribute to elevated conductivity in the SCLM (Duba and Shankland, 1982) given an appropriate network of faults/joints along which the charge carriers may diffuse. Carbon in graphite form behaves electrically as a metal and therefore has very high electrical conductivity, typically 10^5 S/m (Duba and Shankland, 1982). Graphite is an accessory phase in many xenoliths observed worldwide (Pearson et al., 1994). We suggest a combination of graphite and possibly grain boundary carbon are the most attractive explanations for the source of the conductivity enhancement within the upper mantle.

Craven et al. (2001), following Foley (1988), suggest a redox melting model for emplacing graphite in the lithosphere as a consequence of plume and plate tectonic processes during Meso- and Neoarchean times. Given that Fe^{3+} is generally incompatible, then geochemical depletion and 'redox melting' are coupled processes, and MT may therefore identify regions where ancient C-H fluid-present partial melting occurred under reducing or depleted conditions. In the highly anisotropic regions of the western Superior Province, the graphite residual from syn- to post-tectonic partial melting may have been deposited along the (weak) fault zones, and thus explains the parallelism between the MT anisotropy directions and major zones of transpression. Within the Slave craton, the direct spatial correlation of the Central Slave Mantle Conductor with the ultradepleted zone of Griffin et al. (1999) suggests 'redox' processes.

10. Conclusions

Area selection for potentially diamondiferous provinces in frontier regions is problematic given the lack of a predictive model. Accordingly, one needs to acquire data indicative of such provinces, and herein we proposed that deep probing MT surveys can address the three fundamental questions that need to be answered. Is the region old? Is the lithosphere thick? Does the lithosphere contain observable amounts of carbon? MT is a powerful technique, especially when coupled with appropriate teleseismic studies. MT surveys have the advantage that the technique is sensitive to electronic conduction in carbon (when in graphite form), and that the data acquisition generally requires only 1 month per site, rather than the 1 to 2 years that is required for teleseismic surveys.

Examples have been shown of the electrical geometries of the Slave craton and the western part of the Superior craton. In contrast, Rae craton mantle lithosphere around Baker Lake does not contain any observable conductivity enhancements, thus excluding interconnected graphite or grain boundary carbon. Taking the points presented in this paper, we suggest that

1. the central part of the Slave craton west of the Pb isotope boundary is likely to be as productive as the Lac de Gras Corridor of Hope,
2. the North Caribou Terrane of western Superior Province is also likely to be as productive, and
3. the Rae craton around Baker Lake will not yield high quantities of diamonds.

Of course, (1) and (2) are predicated on kimberlites successfully bringing the diamonds to the surface.

Acknowledgements

The Slave craton and Western Superior province work was made possible through the efforts of many people. We gratefully acknowledge the logistical and financial support of Lithoprobe, Geological Survey of Canada, National Science Foundation's Continental Dynamics program, Indian and Northern Affairs Canada, De Beers Canada Exploration, Kennecott Canada Exploration, Diavik Diamond Mines, BHP Billiton Diamonds, Falconbridge, Royal Oak Mines and Miramar Mining. Reviews of an earlier draft of this manuscript by B. Corner and G.H. Read are gratefully acknowledged. Geological Survey of Canada publication 2004044. Lithoprobe publication 1368. Dublin Institute for Advanced Studies publication GP165.

References

Alard, O., Griffin, W.L., Lorand, J.P., Jackson, S.E., O'Reilly, S.Y., 2000. Non-chondritic distribution of the highly siderophile elements in mantle sulphides. Nature 407, 891–894.

Alekseyev, A.S., Vanyan, L.L., Berdichevsky, M.N., Nikolayev, A.V., Okulessky, B.A., Ryaboy, V.Z., 1977. Map of asthenospheric zones of the Soviet Union. Dokl. Akad. Nauk 234, 22–24.

Bahr, K., Simpson, F., 2002. Electrical anisotropy below slow- and fast-moving plates: paleoflow in the upper mantle? Science 295, 1270–1272.

Bailey, R.C., 1970. Inversion of the geomagnetic induction problem. Proc. R. Soc. Lond., Ser. A 315, 185–194.

Beblo, M., 1982. Electrical conductivity of minerals and rocks at ordinary temperatures and pressures. Numerical Data and Functional Relationships in Science and Technology. Group V: Geophysics and Space Research, vol. 1. Physical Properties of Rocks, Springer, Berlin, pp. 239–253. Chapter. 5.1.

Bleeker, W., 2002. Archean tectonics: a review, with illustrations from the Slave craton. In: Fowler, C.M.R., Ebinger, C.J., Hawkesworth, C.J. (Eds.), The Early Earth, Physical, Chemical and Biological Development. Special Publication - Geological Society of London, vol. 199, pp. 151–181.

Boerner, D.E., Kurtz, R.D., Craven, J.A., Ross, G.M., Jones, F.W., Davis, W.J., 1999. Electrical conductivity in the Precambrian lithosphere of Western Canada. Science 283, 668–670.

Calcagnile, G., 1982. The lithosphere–asthenosphere system in Europe. Tectonophysics 90, 19–35.

Calcagnile, G., 1991. Deep structure of Fennoscandia from fundamental and higher mode dispersion of Rayleigh waves. Tectonophysics 195, 139–149.

Calcagnile, G., Panza, G.F., 1987. Properties of the lithosphere–asthenosphere system in Europe with a view towards Earth conductivity. Pure Appl. Geophys. 125, 241–254.

Clifford, T.N., 1966. Tectono-magmatic-units, metallogenic provinces of Africa. Earth Planet. Sci. Lett. 1, 421–434.

Constable, S., Heinson, G., 1993. In defence of a resistive oceanic upper mantle: reply to comment by Tarits Chave and Schultz. Geophys. J. Int. 114, 717–723.

Constable, S.C., Parker, R.L., Constable, C.G., 1987. Occam's inversion: a practical algorithm for generating smooth models from electromagnetic sounding data. Geophysics 52, 289–300.

Cousens, B.L., Aspler, L.B., Charenzelli, J.R., Donaldson, J.A., Sendeman, H., Peterson, A.D., LeCheminant, A.N., 2001. Enriched Archean lithospheric mantle beneath Western churchill province tapped during paleoproterozoic orogenesis. Geology 29, 827–830.

Craven, J.C., Kurtz, R.D., Boerner, D.E., Skulski, T., Spratt, J., Ferguson, I.J., Wu, X., Bailey, R.C., 2001. Conductivity of western Superior Province upper mantle in northwestern Ontario. Curr. Res. - Geol. Surv. Can. (2001-E6, 6 pp.).

Davies, G.F., 1992. On the emergence of plate tectonics. Geology 20, 963–966.

Davis, W.J., Hegner, E., 1992. Neodymium isotopic evidence for the accretionary development of the Late Archean Slave Province. Contrib. Mineral. Petrol. 111, 493–504.

Davis, W.J., Jones, A.G., Bleeker, W., Grütter, H., 2003. Lithospheric development in the Slave Craton: a linked crustal and mantle perspective. Lithos 71, 575–589.

deGroot-Hedlin, C., Constable, S., 1990. Occam's inversion to generate smooth two-dimensional models from magnetotelluric data. Geophysics 55, 1613–1624.

Drury, M.R., Fitz Gerald, J.D., 1996. Grain boundary melt films in an experimentally deformed olivine-orthopyroxene rock; implications for melt distribution in upper mantle rocks. Geophys. Res. Lett. 23, 701–704.

Duba, A.L., Shankland, T.J., 1982. Free carbon and electrical conductivity in the Earth's mantle. Geophys. Res. Lett. 9, 1271–1274.

Ducea, M.N., Park, S.K., 2000. Enhanced mantle conductivity from sulfide minerals, southern Sierra Nevada, California. Geophys. Res. Lett. 27, 2405–2408.

Fischer, G., Le Quang, B.V., 1981. Topography and minimization of the standard deviation in one-dimensional magnetotelluric modelling. Geophys. J. R. Astron. Soc. 67, 279–292.

Foley, S.F., 1988. The genesis of continental basic alkaline magmas—an interpretation in terms of redox melting. J. Petrol. Spec. Lithos. 139–161.

Garcia, X., Jones, A.G., 2001. Decomposition of three-dimensional magnetotelluric data. In: Zhdanov, M.S., Wannamaker, P.E. (Eds.), Three-Dimensional Electromagnetics. Methods in Geochemistry and Geophysics, vol. 35. Elsevier, Amsterdam, pp. 235–250. ISBN 0 444 50429 X.

Griffin, W.L., Ryan, C.G., 1995. Trace elements in indicator minerals: area selection and target evaluation in diamond exploration. In: Griffin, L. (Ed.), Diamond Exploration into the 21st Century. J. Geochem. Explor., vol. 53, pp. 311–337.

Griffin, W.L., Doyle, B.J., Ryan, C.G., Pearson, N.J., O'Reilly, S., Davies, R., Kivi, K., van Achterbergh, E., Natapov, L.M., 1999. Layered mantle lithosphere in the Lac de Gras area, Slave craton: composition, structure and origin. J. Petrol. 40, 705–727.

Groom, R.W., Bailey, R.C., 1989. Decomposition of magnetotelluric impedance tensors in the presence of local three-dimensional galvanic distortion. J. Geophys. Res. 94, 1913–1925.

Groom, R.W., Kurtz, R.D., Jones, A.G., Boerner, D.E., 1993. A quantitative methodology for determining the dimensionality of conductive structure from magnetotelluric data. Geophys. J. Int. 115, 1095–1118.

Grütter, H.S., Apter, D.B., Kong, J., 1999. Crust–mantle coupling; evidence from mantle-derived xenocrystic garnets. In: Dawson, J.B. (Ed.), Proc. 7th International Kimberlite Conference, Conference Proceedings University of Cape Town, South Africa, vol. 1, pp. 307–313.

Gurney, J.J., Zweistra, P., 1995. The interpretation of the major element compositions of mantle minerals in diamond exploration. In: Griffin, W.L. (Ed.), Diamond exploration into the 21st century. J. Geochem. Explor., vol. 53, pp. 293–309.

Haak, V., 1982. Electrical conductivity of minerals and rocks at high temperatures and pressures. Numerical Data and Functional Relationships in Science and Technology. Group V: Geophysics and Space Research, vol. 1. Physical Properties of Rocks, Springer, Berlin, pp. 291–307. Chapter 5.5.

Hamilton, W.B., 1998. Archean magmatism and deformation were not products of plate tectonics. Precambrian Res. 91, 143–179.

Helmstaedt, H.H., Gurney, J.J., 1995. Geotectonic controls of primary diamond deposits; implications for area selection. In: Griffin, W.L. (Ed.), Diamond Exploration into the 21st century. J. Geochem. Explor., vol. 53, pp. 125–144.

Hirth, G., Evans, R.L., Chave, A.D., 2000. Comparison of conti-

nental and oceanic mantle electrical conductivity: is the Archean lithosphere dry? Geochem. Geophys. Geosyst. 1 (Article, 2000GC000048).

Jaupart, C., Mareschal, J.C., 1999. The thermal structure and thickness of continental roots. In: van-der-Hilst, R.D., McDonough, W.F. (Eds.), Composition, Deep Structure and Evolution of Continents. Lithos, vol. 48, pp. 93–114.

Jennings, C.M.H., 1995. The exploration context for diamonds. In: Griffin, W.L. (Ed.), Diamond Exploration into the 21st Century. J. Geochem. Explor., vol. 53, pp. 113–124.

Jones, A.G., 1982. On the electrical crust–mantle structure in Fennoscandia: no Moho and the asthenosphere revealed? Geophys. J. R. Astron. Soc. 68, 371–388.

Jones, A.G., 1998. Waves of the future: superior inferences from collocated seismic and electromagnetic experiments. Tectonophysics 286, 273–298.

Jones, A.G., 1999. Imaging the continental upper mantle using electromagnetic methods. Lithos 48, 57–80.

Jones, A.G., Ferguson, I.J., 2001. The electric moho. Nature 409, 331–333.

Jones, A.G., Garcia, X., 2003. The Okak Bay MT dataset case study: a lesson in dimensionality and scale. Geophysics 68, 70–91.

Jones, A.G., Ferguson, I.J., Chave, A.D., Evans, R., McNeice, G.W., 2001. The electric lithosphere of the Slave craton. Geology 29, 423–426.

Jones, A.G., Snyder, D., Hanmer, S., Asudeh, I., White, D., Eaton, G., Clarke, G., 2002. Magnetotelluric and teleseismic study across the Snowbird Tectonic Zone, Canadian shield: a neoarchean mantle suture? Geophys. Res. Lett. 29 (17), 10-1–10-4 (doi: 10.1029/2002GL015359).

Jones, A.G., Lezaeta, P., Ferguson, I.J., Chave, A.D., Evans, R.L., Garcia, X., Spratt, J., 2003. The electrical structure of the Slave craton. Lithos 71, 505–527.

Kay, I., Sol, S., Kendall, J.-M., Thomson, C., White, D., Asudeh, I., Roberts, B., Francis, D., 1999. Shear wave splitting observations in the Archean Craton of Western Superior. Geophys. Res. Lett. 26, 2669–2672.

Kopylova, M.G., Russel, J.K., Cookenboo, H., 1997. Petrology of peridotite and pyroxenite xenoliths from Jericho Kimberlite; implications for the thermal state of the mantle beneath the Slave Craton, northern Canada. J. Petrol. 40, 79–104.

Kopylova, M.G., Caro, G., Russell, J.K., 2001. Kimberlite and xenoliths from the Southern Slave—a terrain with the highest diamond potential in the Slave craton. In: Cook, F., Erdmer, P. (comp), Slave-Northern Cordillera Lithospheric Evolution (SNORCLE) Transect and Cordilleran Tectonics Workshop Meeting (February 22–25), Pacific Geoscience Centre Sidney, BC Lithoprobe Report No. 79, 18–24.

Ledo, J., Jones, A.G., 2003. Temperature bounds of the Intermontane Belt mantle (northern Canadian Cordillera) using its mineral composition and electrical conductivity. Presented at the European Geophysical Society–European Union of Geosciences–American Geophysical Union joint meeting, Nice, France, April, 6–11.

Lewis, T.J., Hyndman, R., 1998. Heat flow transitions along the SNORCLE Transect; asthenospheric flow. In: Slave-NORthern Cordillera Lithospheric Evolution (SNORCLE) and Cordilleran tectonics workshop. Compiled by: F. Cook and P. Erdmer-Philippe. Lithoprobe Report 64, 92.

MacKenzie, J.M., Canil, D., 1999. Composition and thermal evolution of cratonic mantle beneath the central Archean Slave Province NWT, Canada. Contrib. Mineral. Petrol. 134, 313–324.

Macnae, J.C., 1995. Applications of geophysics for the detection and exploration of kimberlites and lamproites. In: Griffin, W.L. (Ed.), Diamond Exploration into the 21st Century. J. Geochem. Explor., vol. 53, pp. 213–243.

Mareschal, M., Kellett, R.L., Kurtz, R.D., Ludden, J.N., Bailey, R.C., 1995. Archean cratonic roots, mantle shear zones and deep electrical anisotropy. Nature 373, 134–137.

McKenzie, D.P., Bickle, M.J., 1988. Volume and composition of melt generated by extension of the lithosphere. J. Petrol. 29, 625–679.

McNeice, G., Jones, A.G., 2001. Multisite, multifrequency tensor decomposition of magnetotelluric data. Geophysics 66, 158–173.

Meju, M., 2002. Geoelectromagnetic exploration for natural resources: models, case studies and challenges. Surv. Geophys. 23, 133–206.

Minarik, W.G., Watson, E.B., 1995. Interconnectivity of carbonate melt at low melt fraction. Earth Planet. Sci. Lett. 133, 423–437.

Morgan, P., 1995. Diamond exploration from the bottom up: regional geophysical signatures of lithosphere conditions favorable for diamond exploration. In: Griffin, W.L. (Ed.), Diamond Exploration into the 21st Century. J. Geochem. Explor., vol. 53, pp. 145–165.

Partzsch, G.M., Schilling, F.R., Arndt, J., 2000. The influence of partial melting on the electrical behavior of crustal rocks: laboratory examinations, model calculations and geological interpretations. Tectonophysics 317, 189–203.

Pearson, D.G., Boyd, F.R., Haggerty, S.E., Pasteris, J.D., Field, S.W., Nixon, P.H., Pokhilenko, N.P., 1994. The characterisation and origin of graphite in cratonic lithospheric mantle: a petrological carbon isotope and Raman spectroscopic study. Contrib. Mineral. Petrol. 115, 449–466.

Pearson, N.J., Griffin, W.L., Doyle, B.J., O'Reilly, S.Y., Van Achterbergh, E., Kivi, K., 1999. Xenoliths from kimberlite pipes of the Lac de Gras area, Slave craton, Canada. In: Gurney, J.J., et al., (Ed.), Proceedings of the 7th International Kimberlite Conference, P.H. Nixon Volume 2: Red Roof Design, Cape Town, pp. 644–658.

Rodi, W., Mackie, R.L., 2001. Nonlinear conjugate gradients algorithm for 2-D magnetotelluric inversion. Geophysics 66, 174–187.

Russell, J.K., Kopylova, M.G., 1999. A steady-state conductive geotherm for the north-central Slave: inversion of petrological data from the Jericho kimberlite pipe. J. Geophys. Res. 104, 7089–7101.

Russell, J.K., Dipple, G.M., Kopylova, M.G., 2001. Heat production and heat flow in the mantle lithosphere to the Slave craton, Canada. Phys. Earth Planet. Inter. 123, 27–44.

Ryan, R.G., Grffin, W.L., Pearson, N.J., 1996. Garnet Geotherms: a technique for derivation of $P-T$ data from Cr-pyrope garnets. J. Geophys. Res. 101, 5611–5625.

Schilling, F.R., Partzsch, G.M., Brasse, H., Schwarz, G., 1997.

Partial melting below the magmatic arc in the central Andes deduced from geoelectromagnetic field experiments and laboratory data. Phys. Earth Planet. Inter. 103, 17–31.

Schultz, A., Kurtz, R.D., Chave, A.D., Jones, A.G., 1993. Conductivity discontinuities in the upper mantle beneath a stable craton. Geophys. Res. Lett. 20, 2941–2944.

Simpson, F., 2001. Resistance to mantle flow inferred from the electromagnetic strike of the Australian upper mantle. Nature 412, 632–634.

Siripunvaraporn, W., Egbert, G., 2000. An efficient data-subspace inversion method for 2-D magnetotelluric data. Geophysics 65, 791–803.

Smith, J.T., Booker, J.R., 1988. Magnetotelluric inversion for minimum structure. Geophysics 53, 1565–1576.

Smith, J.T., Booker, J.R., 1991. Rapid inversion of two and three-dimensional magnetotelluric data. J. Geophys. Res. 96, 3905–3922.

Snyder, D.B., Bostock, M.G., Lockhart, G.D., 2004. Mapping the mantle lithosphere for diamond potential using teleseismic methods. Lithos. 77, 859–872 doi:10.1016/j.lithos.2004.03.049.

Thorpe, R.I., Cumming, G.L., Mortensen, J.K., 1992. A significant Pb isotope boundary in the Slave Province and its probable relation to ancient basement in the western Slave Province. Project Summaries, Canada-Northwest Territories Mineral Development Subsidiary Agreement. Open File Rep. - Geol. Surv. Can., vol. 2484, pp. 279–284.

Vozoff, K., 1972. The magnetotelluric method in the exploration of sedimentary basins. Geophysics 37, 98–141.

Vozoff, K. (Ed.), 1986. Magnetotelluric Methods. Soc. Explor. Geophys. Reprint Ser. No. 5: Tulsa, OK, ISBN 0-931830-36-2.

Vozoff, K., 1991. The magnetotelluric method. Electromagnetic Methods in Applied Geophysics—Applications. Soc. Explor. Geophys., pp. 641–712. Tulsa, OK, Chapter 8.

Wannamaker, P.E., Hohmann, G.W., Ward, S.H., 1984. Magnetotelluric responses of three-dimensional bodies in layered earths. Geophysics 49, 1517–1533.

Wannamaker, P.E., Stodt, J.A., Rijo, L., 1985. PW2D: Finite Element Program for Solution of Magnetotelluric Responses of Two-Dimensional Earth Resistivity Structure. Earth Sci. Lab. Univ. Utah Res. Inst, Salt Lake City.

White, D.J., Musacchio, G., Helmstaedt, H.H., Harrap, R.M., Thurston, P.C., van der Velden, A., Hall, K., 2003. Images of a lower-crustal oceanic slab: direct evidence for tectonic accretion in the Archean western Superior province. Geology 31, 997–1000.

Xu, Y., Shankland, T.J., Poe, B.T., 2000. Laboratory-based electrical conductivity of the Earth's mantle. J. Geophys. Res. 105, 27865–27875.